Structural Analysis of Cellulose Acetate and Zirconium Alkoxide Hybrid Fibers

Hanako Asai[1,*] Hiroaki Nitani[2], Fumihiro Nishimura[3], Susumu Yonezawa[3] and Koji Nakane[1]

[1] Frontier Fiber Technology and Science, Graduate School of Engineering, University of Fukui, 3-9-1 Bunkyo, Fukui, 910-8507, Japan.

[2] Institute of Materials Structure Science, High Energy Accelerator Research Organization (KEK), 1-1 Oho, Tsukuba, Ibaraki 305-0801, Japan

[3] Headquarters for Innovative Society-Academia Cooperation, University of Fukui, 3-9-1 Bunkyo, Fukui, 910-8507, Japan

1 Introduction

Cellulose acetate (CA)-Zr hybrid materials have attracted attention for their applications as absorbents for chemical separations or supports for enzyme immobilizations.[1-9] CA can be easily molded into different forms, such as membranes and fibers,[10] and zirconia is known to have great chemical resistance, thermal stability, permeability and biocompatibility compared to silica, alumina and titania,[4,9] and it has phosphate ion absorption ability.[8] CA can form composite materials with zirconia, via coordination of – OH or –CO groups to zirconium species.[4, 8] For example, the report of Rodrigues-Filho et al. shows that CA-Zr composite membranes can act as absorbents for phosphate chemical species, which cause serious algae proliferation and environmental problems.[8] They prepared the membrane by immersing CA cast film into a zirconium alkoxide $(Zr(OR)_4)$ solution. In contrast, Nakane et al. studied fibrous CA-Zr composites for enzyme immobilization, preparing them by injecting CA solution into a $Zr(OR)_4$ bath using an air-gap spinning technique.[3-6] CA chains are instantaneously cross-linked by $Zr(OR)_4$, from which fibrous gels can be obtained. By using $Zr(OR)_4$, the gel becomes tough enough to resist high pressure in an enzyme reaction column.[4] In addition, as fibrous materials have larger surface areas than film materials, fibrous CA-Zr composites should be more efficient phosphate ion absorbents and superior supports for enzyme immobilization. In addition, CA-Zr or cellulose-Zr composites can be converted into CA-zirconium phosphate composites,[10] which have been studied as ion-exchange materials.[2, 11]

However, in spite of the many application studies, it is still unclear how preparation conditions influence the structure of CA-Zr gel fibers. In this study, we systematically investigated the effect of alkyl chain length and $Zr(OR)_4$ bath concentration on the structure of resultant CA-Zr fibers, using various methods including X-ray absorption fine structure (XAFS) measurements. Zr XAFS is a powerful tool for the analysis of local structure around a target element, allowing us to obtain information on coordination number and bond distance. In addition, We compared the structures of hydrolyzed $Zr(OR)_4$ with and without CA fiber, and studied the effect of confinement to the CA fiber on the structure of Zr. This structural knowledge provided useful information for the preparation of CA-Zr composite materials.

2 Experiment

2.1 Preparation of the CA-Zr(OR)$_4$ fibers and comparison samples

The sample preparation method, a so-called air-gap spinning technique, is schematically represented in Fig. 1. Firstly, a 15 wt% CA-acetone solution was prepared using dehydrated acetone. In another bottle, each $Zr(OR)_4$ compound was dissolved in 15.2 g dehydrated acetone. The CA solution was then set in a syringe with a 21G needle, and ejected by syringe pump into the stirred $Zr(OR)_4$ solution bath, instantaneously forming a fibrous material. After the determined immersion time, the obtained fibers were repeatedly washed with acetone, followed by distilled water, in order to remove unreacted components. All samples were dried under vacuum and used for measurements. The $Zr(OR)_4$ bath concentrations were 1, 2.5, 5, 10, 15, 20, and 25 wt%. The immersion times were 1, 5, 10, 30, and 60 min. The nozzle-to-bath distance, spinning solution volume, and spinning rate were 10 cm, 2.5 mL, and 3 mL min^{-1}, respectively.

Two types of $Zr(OR)_4$ with different alkyl lengths, $Zr(OPr)_4$ and $Zr(OBu)_4$, were used in this study. For comparison, we also prepared a pure CA fiber sample (CA-Zr-0), a hydrolyzed $Zr(OBu)_4$ sample (Bu-H), and a hydrolyzed $Zr(OPr)_4$ sample (Pr-H). CA-Zr-0 was prepared by ejecting 15 wt% CA solution into distilled water. Bu-H and Pr-H was prepared by drying each alkoxide solution in a glass dish.
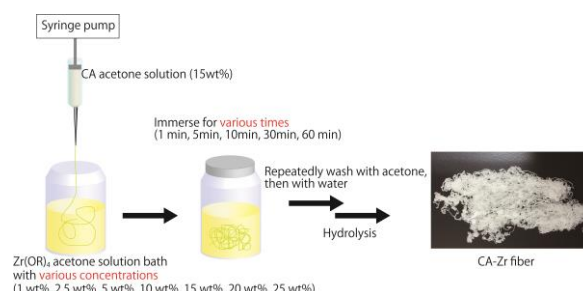

Fig. 1: Schematic representation of CA-Zr fiber preparation methods.

2.2 XAFS measurements.

The prepared fiber samples were pulverized with an agate mortar, and put through a 400-mesh sieve, in order to obtain a homogeneous fine powder. These powdered fiber samples were then compressed into 10 mmϕ pellets together with boron nitride, which acted as a binder. Preliminary proper sample weights were calculated using the residual content values obtained from TGA analysis and SAMPLEM4M software. Zr K-edge XAFS measurements were carried out in transmission mode using synchrotron radiation through a Si(111) monochromator at BL-12C in Photon Factory, Institute of Materials Structure Science, High Energy Accelerator Research Organization (KEK), Japan. XAFS spectra were analysed by Athena and Artemis software.[12] Fourier transformation of k^3-weighted EXAFS oscillation was performed in the range of the wave vector k = 1.8–14 Å^{-1}.

3 Results and Discussion

Fig. 2 shows normalized XANES spectra for the Zr(OBu)$_4$ series, Zr(OPr)$_4$ series, Bu-H, Pr-H, ZrO$_2$, and Zr foil. No differences were observed among the Zr(OBu)$_4$ series, Zr(OPr)$_4$ series, Bu-H, and Pr-H, indicating that their local structures were similar. Fig. 3 shows the Fourier transformed EXAFS spectra for ZrO$_2$, Zr(OBu)$_4$ fiber samples, and Bu-H. The fiber samples and Bu-H produced similar curves, giving strong peaks at 1.6 Å, assigned to the Zr-O bond,[13] and a small peak at 3.1 Å, assigned to the Zr-Zr distance.[14] Both peak positions did not change with increasing Zr(OR)$_4$ concentration, indicating that the distance was not affected by Zr content, even at the upper limit. Therefore, we concluded that Zr(OR)$_4$ was incorporated in its hydrolyzed form, where some Zr species were polymerized and the distance between neighboring Zr atoms was not affected by the Zr content of the whole fiber. The EXAFS curves were similar to those of polymeric Zr hydroxide,[14, 15] suggesting the formation of Zr(OH)$_4$ derivatives in the fiber sample and Bu-H, which was consistent with ATR-FTIR results. In addition, there were no large oscillations in the high length region (above 4 Å) for Zr(OBu)$_4$ fiber samples and Bu-H, in contrast with ZrO$_2$. This result indicated that Zr in the fiber sample and Bu-H did not have a long-period structure, as found in ZrO$_2$, which was consistent with the XRD results.

Next, we performed curve fitting analysis of the EXAFS oscillations for the first coordination sphere of Zr(OBu)$_4$ and Zr(OPr)$_4$ fiber samples. The obtained coordination numbers and Zr-O distances are summarized in Fig. 4. The coordination numbers were near 6, and were not affected by the type of alkoxide or concentration. The obtained coordination numbers for Bu-H and Pr-H were also ca. 6, in agreement with the report of Bradley et al.[16]

Finally, we have depicted the structure of the CA-Zr fiber in Fig. 5. It should be noted that this schematic representation is different from that reported previously.4 Considering the XAFS and ATR-FT-IR results, the Zr contained in the CA fiber is hexacoordinate, and has the same structure as that of hydrolyzed Zr alkoxide, containing Zr-OH. We surmised that the Zr alkoxides in the fiber were polymerized, but the degree of polymerization of hydrolyzed Zr alkoxide was assumed to be small, in accordance with the literature.[16] In addition, considering that condensation reactions should be slower than hydrolysis and gelation reactions,[17] we assumed that, after one Zr(OR)$_4$ molecule forms a cross-linking point with CA chains, a few other Zr(OR)$_4$ molecules become polymerized with that cross-linking Zr(OR)$_4$. The Zr alkoxide type and concentration did not influence the local structure of the cross-linking point.
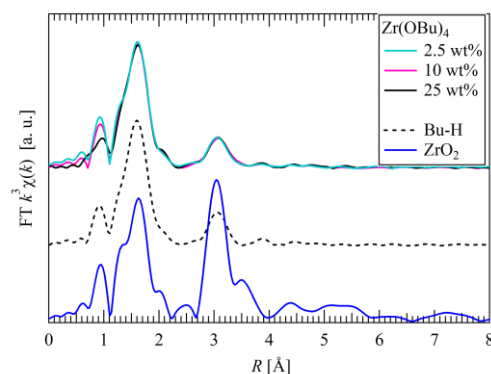

Fig. 3: Fourier-transformed k^3-weighted Zr K-edge EXAFS spectra for CA-Zr fiber samples prepared at different Zr(OBu)$_4$ bath concentrations, Bu-H, and ZrO$_2$.
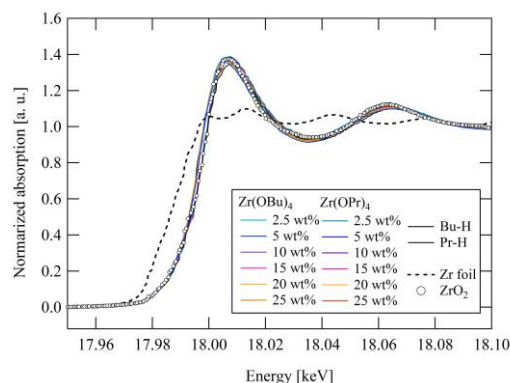

Fig. 2: Normalized XANES spectra for Zr(OBu)$_4$ and Zr(OPr)$_4$ series, Bu-H, Pr-H, Zr foil and ZrO$_2$.
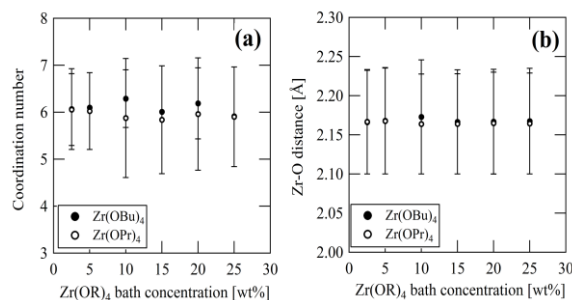

Fig. 4: (a) Coordination numbers and (b) Zr-O distances evaluated from fitting analysis of EXAFS results.
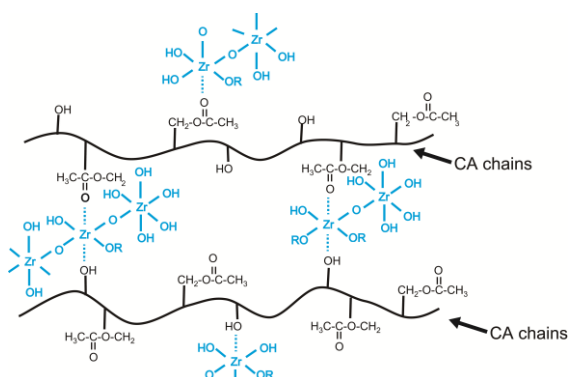
Fig. 5: Schematic representation of the structure of CA-Zr fibers surmised from ATR-FTIR and XAFS results.

4. Conclusions

In this study, we investigated the effects of $Zr(OR)_4$ bath concentration and alkoxide-type on the structure of the CA-Zr fibers obtained. The type of alkoxide did not affect the local structure of CA-Zr fibers, but influenced their gelation speed (faster for $Zr(OPr)_4$). In addition, there was an upper limit to Zr content in the fiber (less than 30 wt%). EDS analysis revealed that for high $Zr(OPr)_4$ bath concentration, Zr was homogeneously distributed inside the fiber, while for low bath concentrations, Zr existed locally at the fiber surface. These results suggested that the gelation reaction proceeded from outside of the fiber. However, in the case of $Zr(OBu)_4$, homogeneous Zr distribution was observed for all $Zr(OBu)_4$ concentrations. These results might be attributed to the differences in reactivity and diffusion speed between the two alkoxides used. Finally, ATR-FTIR and XAFS measurements revealed detailed structural information on the CA-Zr fibers, showing that the Zr species were similar to hydrolyzed $Zr(OR)_4$, and that the local structure-forming cross-linking point was not altered by Zr content and alkoxide type.

References

[1] J. E. Kiefer and G. Touey, *I&EC Product Research and Developement*, **4**, 253 (1965).

[2] V. K. Gupta, D. Pathania, P. Singh, B. S. Rathore and P. Chauhan, *Carbohydrate Polym.*, **95**, 434 (2013).

[3] K. Nakane, S. I. Suye, T. Ueno, Y. Ohno, T. Ishikawa, T. Ogihara and N. Ogata, *J. Appl. Polym. Sci.*, **116**, 2901 (2010).

[4] K. Nakane, T. Ogihara, N. Ogata and Y. Kurokawa, *J. Mater. Res.*, **18**, 672 (2003).

[5] K. Nakane, T. Ogihara, N. Ogata and Y. Kurokawa, *J. Appl. Polym. Sci.*, **81**, 2084 (2001).

[6] Y. Kurokawa, *Polymer Gels and Networks*, **4**, 153 (1996).

[7] S. A. Nabi and M. Naushad, *Colloids and Surfaces A: Physicochem. Eng. Aspects*, **316**, 217 (2008).

[8].U. P. Rodrigues-Filho, Y. Gushikem, M. C. Goncalves, R. C. Cachichi and S. C. Castro, *Chem. Mater.*, **8**, 1375 (1996).

[9] G. Arthanareeswaran and P. Thanikaivelan, *Separation and Purification Technology*, **74**, 230 (2010).

[10] C. A. Borgo, A. M. Lazarin and Y. Gushikem, *Sensors and Actuators B*, **87**, 498 (2002).

[11] C. A. Borgo and Y. Gushikem, *J. Colloid Interface Sci.* , **246**, 343 (2002).

[12] B. Ravel and M. Newville, *J. Synchrotron Rad.*, **12**, 537 (2005).

[13] T. Tobase, A. Yoshiasa, L. Wang, H. Hong, H. Isobe and R. Miyawaki, *J. Mineral. Petrol. Sci.*, **110**, 1-7 (2015).

[14] C. Walther, J. Rothe, M. Fuss, S. Buchner, S. Koltsov and T. Bergmann, *Anal. Bioanal. Chem.*, **388**, 409 (2007).

[15] H. R. Cho, C. Walther, J. Rothe, V. Neck, M. Denecke, K. Dardenne and T. Fanghanel, *Anal. Bioanal. Chem.*, **383**, 28 (2005).

[16] D. C. Bradley and D. G. Carter, *Can. J. Chem.*, **39**, 1434 (1961).

[17] M. J. Percy, J. R. Bartlett, J. L. Woolfrey, L. Spiccia and B. O. West, *J. Mater. Chem.*, **9**, 499 (1999).

* h_asai@u-fukui.ac.jp